Journal of Solution Chemistry (2018) 47:1768–1778
https://doi.org/10.1007/s10953-018-0812-2

Cucurbit[7]uril Inclusion Complexes with Benzimidazole Derivatives: A Computational Study

Samer K. Albdallah[1] · Khaleel I. Assaf[2,3] · Khaled Bodoor[4] · Nada A. Al-Sakhen[1] · Lama D. Malhis[1] · Akef I. Alhmaideen[1] · Musa I. El-Barghouthi[1,5]

Received: 19 February 2018 / Accepted: 8 July 2018 / Published online: 25 September 2018

Abstract
Molecular dynamics (MD) simulations were carried out to study the host–guest complexation in aqueous solution between cucurbit[7]uril (CB7) and the neutral and protonated forms of benzimidazole derivatives. Complexation occurs via encapsulation of the hydrophobic part (benzene ring) of the guest within the CB7 hydrophobic cavity, and the interactions of the amine group(s) of the imidazole ring of the guest with the CB7 carbonyl portals. The molecular mechanics Poisson–Boltzmann surface area (MM-PBSA) method is used to estimate the host–guest Gibbs energy of binding. The results indicate that CB7 binds the protonated form more strongly than the neutral one, and that the dominant contribution to the Gibbs energy of complexation for the neutral and protonated guests is associated, respectively, with the host–guest van der Waals and electrostatic interactions. Quantum chemical calculations using dispersion-corrected density functional theory (DFT) are used to calculate the binding affinities and to predict the pK_a values of the free and complexed guests. The calculated pK_a values for the free guests reveal excellent agreement with the experimental values, while for the complexed guests, general trends are obtained.

Keywords Macrocycles · MD-simulations · MM-PBSA · Inclusion complexes

✉ Khaleel I. Assaf
k.assaf@jacobs-university.de

✉ Khaled Bodoor
kbodoor@ju.edu.jo

✉ Musa I. El-Barghouthi
musab@hu.edu.jo

[1] Department of Chemistry, The Hashemite University, P.O. Box 150459, Zarqa 13115, Jordan

[2] Department of Life Sciences and Chemistry, Jacobs University Bremen, Campus Ring 1, 28759 Bremen, Germany

[3] Department of Chemistry, Faculty of Science, Al-Balqa Applied University, P.O. Box 19117, Al-Salt, Jordan

[4] Department of Physics, The University of Jordan, Amman 11942, Jordan

[5] Department of Chemistry, Isra University, Amman 11622, Jordan

1 Introduction

Cucurbit[*n*]urils (CB*n*, *n* = 5–8, 10) are a family of water-soluble macrocyclic host molecules, consisting of *n* glycoluril units linked through methylene bridges [1–4]. They are known to bind neutral and cationic organic guests in aqueous solutions with high affinity [5–8] via a combination of hydrophobic and electrostatic interactions [9–11]. Within the CB*n* family, CB7 is the homologue with most applications due to its high water-solubility and intermediate cavity size, and its ability to bind a wider variety of guest molecules with extraordinary association constants [10, 11]. The CB*n* are used in many applications, including dye tuning, as catalysts, molecular switches and drug binding and delivery [9, 12, 13].

Benzimidazole (BZ) and its derivatives, viz. albendazole (ABZ), carbendazim (CBZ), thiabendazole (TBZ), and fuberidazole (FBZ) (Scheme 1), are known as being fungicides and anthelmintic drugs [14, 15]. In general, benzimidazoles have limited water solubility and may undergo chemical and photo-degradation [16]. It is well-known that their encapsulation within macrocyclic molecules, such as CBs and cyclodextrins (CDs), enhances their solubility as well as thermal and photochemical stability [17–20]. Furthermore, host–guest complexation can alter the protonation of guest molecules with ionizable groups, which is known as complexation-induced pK_a shifts [13, 18, 20]. These shifts in pK_a values can be exploited to activate pro-drug molecules, stabilize the active form of drug molecules, enhance their solubility, and increase their degree of ionization [13, 18, 20]. Nau and co-workers have reported that the binding for drug molecules with CB7 enhances the stability of the active form through complexation induced protonation [6]. Koner et al. studied the complexation between CB7 and BZ derivatives in aqueous solution, and found complexation-induced shifts in their pK_a values, enhanced water solubility and chemical stability, as well as altered photo-physical properties [18].

Molecular dynamics (MD) simulations and quantum-chemical calculations have been widely used to study CB*n* host–guest complexation [21–29]. Olivia and co-workers have recently applied constant-pH MD simulation (CpHMD) protocol to investigate the pH dependent binding of BZ and its derivatives to CB7 and estimate the induced pK_a shifts; they obtained good agreement with the experimentally reported values, with absolute errors less than 5.4 kJ·mol^{-1} [30]. Fatiha et al. have employed the HF/6-31G and B3LYP/6-31G methods to compare two binding modes of CBZ with CB7, with the benzimidazole and carbamate moieties, respectively, introduced into the CB7 cavity, and found that the

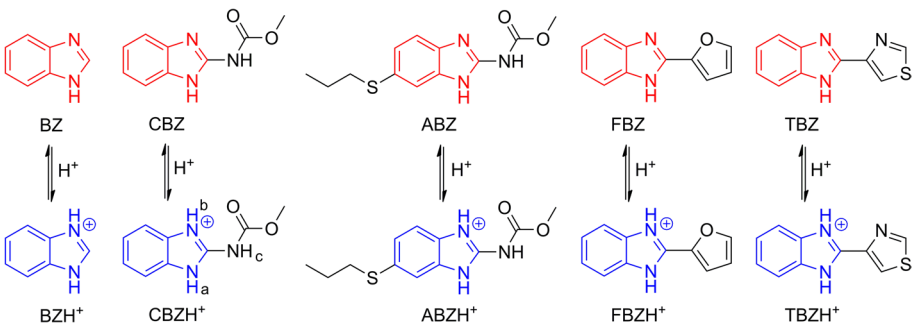

Scheme 1 Chemical structures of the investigated guest molecules

former resulted in a more stable conformation [31]. Shewale et al. have used dispersion-corrected DFT calculations to study the CB7 complexes with BZ and its derivatives (ABZ, CBZ, FBZ and TBZ) and found that inclusion of the benzimidazole moiety resulted in increased binding stability in the following order: ABZ > CBZ > BZ > FBZ ~ TBZ [32].

In this work, MD simulations are used to study the dynamics of the inclusion complexes formed in aqueous solution between CB7 and the protonated and neutral forms of benzimidazole derivatives (Scheme 1). Free binding energies are estimated using the molecular mechanics Poisson–Boltzmann surface area (MM-PBSA) method. Finally, DFT is used to estimate the pK_a values for the guests in their free and bound states. A comparison of both MD and quantum mechanical approaches is made and discussed.

2 Computational Methods

The initial molecular geometry of CB7 was obtained from its experimental XRD structure [2]. Optimized structures for the guest molecules were generated using ab initio (HF/6-31G*) calculations, in order to use them as starting geometries for the MD simulations and to calculate the electrostatic potentials. The initial host–guest complexes, generated by manually inserting the guest into the desired position inside the host cavity, are shown in Scheme 2. MD simulations were performed with the sander module of the AMBER program [33] employing the general amber force field (GAFF) parameter set [34]. RESP charges were used for the atomic charges of the host and guest molecules generated from the electrostatic potentials calculated using an ab initio (HF/6-31G*) method [35]. Each system was solvated in a truncated octahedral periodic box of TIP3P water molecules [36]. Chloride ions were added to maintain the charge neutrality of each system. The non-bonded cut-off was set to 12.0 Å. Prior to starting the MD simulation, each solvated complex was subjected to energy minimization using the conjugate gradient algorithm, followed by gradual heating up to 298 K for 60 ps, and 500 ps of equilibration at 1 atm (1.01325 MPa). During the minimization and production runs, the Particle Mesh Ewald method (PME) was employed to treat the long-range electrostatic interactions in periodic boundary conditions [37]. All bond lengths involving hydrogen atoms were constrained by means of the SHAKE Algorithm [38]. Production runs were carried out for 20 ns at 298 K and 1.0 atm (1.01325 MPa), using 2 fs time steps, saving structures every 2 ps, and updating the non-bonded pair list every 25 steps. Trajectories were analyzed with the PTRAJ module of the AMBER 11 program. The VMD 1.8.6 program was used to visualize the structures [39] The MM-PBSA method and normal mode analysis were employed according to the procedure described elsewhere [21, 22, 24, 40]. For the quantum calculations

Scheme 2 Initial geometry of a typical host–guest inclusion complex

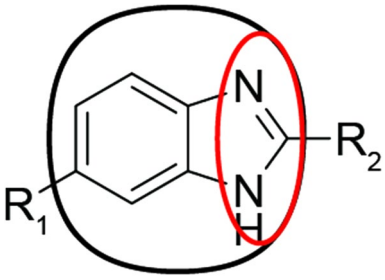

(geometry optimization and binding energy calculations), the dispersion-corrected DFT method (wB97XD/6-31G*) in Gaussian 09 was used, with default convergence criteria. Minima were characterized by the absence of imaginary frequencies. The polarizable continuum model (PCM) was implemented to simulate the effect of solvent [41]. For the pK_a calculations, the procedure was adopted from the literature [42, 43].

3 Results and Discussion

The starting structures for the MD simulations of the complexes had the benzimidazole ring of the guest at the center of the host (Scheme 2). Figure 1 shows for each complex a superposition of representative samples (snapshots) extracted from its 20 ns trajectory. These snapshots revealed complete inclusion of the benzene ring, thus allowing maximum van der Waals interactions with the hydrophobic cavity of CB7. The snapshots for ABZ on the other hand showed only a partial inclusion of the benzene ring and a complete inclusion of the hydrophobic propyl-thio moiety. The imidazole ring in all guests was positioned next to the carbonyl portals, interacting via hydrogen bonds as well as ion–dipole interactions in the case of the protonated guests. The R_2 substituents in all guests were excluded from the cavity and exposed to the surrounding water. The protonated guests assumed more restricted conformations compared to the neutral forms, a result of the strong ion–dipole interactions. Our results are in agreement with the ^{1}H-NMR data obtained by Koner et al. [18] in acidic medium. Specifically, the ^{1}H NMR spectra revealed the encapsulation of the benzimidazole moiety of the guest inside the CB7 cavity, except for ABZH$^+$, in which the hydrophobic propyl-thio moiety shuttles inside CB7.

4 Hydrogen Bond Analysis

A summary of the intermolecular hydrogen bonds (HB) between the guest molecules and the carbonyl oxygens on the CB7 portals is presented in Table 1. The hydrogen bond analysis was carried out using the PTRAJ module of the AMBER 11 program, using a hydrogen

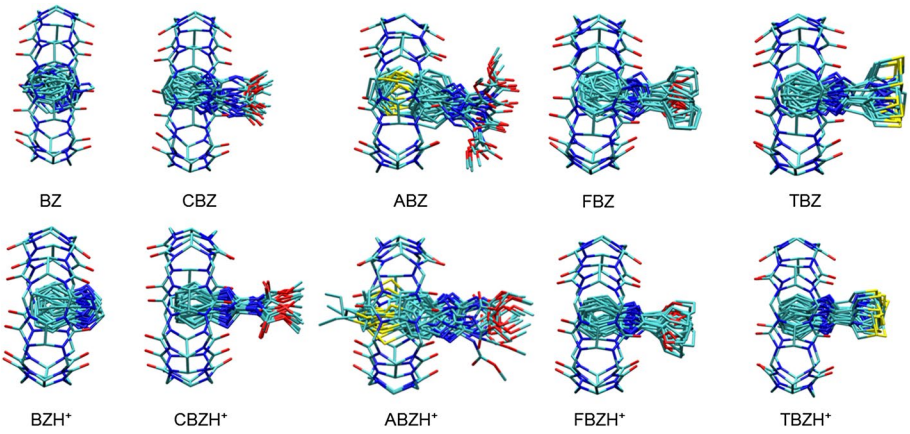

Fig. 1 Dynamics of studied guests shown as a clustered molecular display

Table 1 Hydrogen bond analysis between guests and CB7

Hydrogen	BZ	BZH^+	CBZ	$CBZH^+$	ABZ	$ABZH^+$	FBZ	$FBZH^+$	TBZ	$TBZH^+$
H_a	0.14	0.53	0.05	0.52	0.74	0.66	0.58	0.58	0.60	0.60
H_b	–	0.54	–	0.45	–	0.18	–	0.50	–	0.40
H_c	–	–	0.80	0.00	0.00	0.00	–	–	–	–
Total	0.14	1.07	0.85	0.97	0.74	0.84	0.58	1.08	0.60	1.00

See Scheme 1 for the hydrogen atom labeling

Reported values represent average number of hydrogen bonds per frame

bond cut off distance < 3.2 Å and an angle > 120°. The analysis showed that the protonated guest partakes in more hydrogen bonds than its neutral from, a result of the additional hydrogen atom on the imine group (see Table 1). The enhancement was more pronounced for BZH^+, as this guest adopted a more rigid conformation inside the cavity (Fig. 1). For CBZ, the amide group on the side can also form hydrogen bonds with the carbonyl rim, but not after protonation of the amine/imine groups in the imidazole ring which acts as a stronger competitor (Fig. 1). This resulted in a reduction of the number of hydrogen bonds on H_c from 0.8 to 0 upon protonation of the amine group in the imidazole ring.

5 MM/PBSA Results

Table 2 displays the various contributions to the binding Gibbs energy of each complex as estimated by the MM-PBSA method. The higher Gibbs energy for the protonated form is a direct consequence of the increased electrostatic interactions, with $-\Delta E_{ELE}$ being greater by ~ 209 kJ·mol^{-1} than for the neutral form. The contribution from the van der Waals interaction (ΔE_{VDW}) did not differ much between the two forms, since the same part of the guest is responsible for binding inside the CB cavity. ABZ had the highest $-\Delta E_{VDW}$ value (both forms), due to the encapsulation of the additional thiol residue. ΔG_{NP} values for all complexes of both forms were slightly favorable, ~ − 8 kJ·mol^{-1}, with the small differences between the two forms consistent with their similar binding modes. The solvation energy (ΔG_{solv}) was found to be unfavorable for all complexes: ~ 62–105 and 247–271 kJ·mol^{-1} for the neutral and protonated forms, respectively, with BZH^+ having the largest (ΔG_{solv}) value as a result of its complete inclusion within the CB7 cavity. For all complexes, the large gas-phase interaction energies were largely compensated by the large solvation penalty. Overall, the ΔG values were negative, indicating favorable binding for the guests to CB7. The $-\Delta G$ values for the protonated guests were again much higher than those for the neutral ones. The highest and lowest binding Gibbs energies for the neutral (protonated) forms belonged to ABZ ($ABZH^+$) and BZ (BZH^+). Normal mode calculations yielded negative values of $T\Delta S$ for all complexes, indicating overall reduction in guest and host freedom upon complexation, with the complexes of ABZ and $ABZH^+$ showing the most negative values. This may be due to the different modes of binding with CB7 found for neutral and protonated ABZ (Fig. 1).

The fluctuations in the electrostatic contribution to the complex stability for protonated guests were lower than their neutral analogues (Table 2), in accord with the more restricted conformations adopted by the protonated guests as a result of their strong

Table 2 MM-PBSA estimates of the binding Gibbs energies of the complexes and their decompositions, all in kJ·mol^{-1}

	ΔE_{ELE}	ΔE_{VDW}	ΔE_{INT}	ΔE_{GAS}	ΔG_{NP}	ΔG_{PB}	ΔG_{SOLV}	ΔG	$T\Delta S$	ΔG_{TOT}
BZ	−30.71 (24.64)	−109.91 (12.93)	10.71 (33.89)	−129.91 (43.85)	−7.87 (0.17)	93.68 (25.90)	85.81 (25.90)	**−44.10 (50.92)**	−53.51 (4.69)	9.41 (51.13)
ABZ	−32.17 (15.27)	−137.07 (12.01)	8.33 (34.85)	−160.92 (39.92)	−10.67 (0.21)	97.49 (10.71)	86.82 (10.71)	**−74.10 (41.34)**	−70.71 (1.84)	−3.39 (41.38)
CBZ	−55.02 (14.43)	−123.51 (11.92)	7.99 (35.65)	−170.54 (40.25)	−9.25 (0.25)	113.85 (16.11)	104.60 (16.11)	**−65.94 (43.35)**	−48.53 (4.77)	−17.41 (43.60)
FBZ	−13.35 (16.69)	−109.96 (12.30)	10.13 (34.60)	−113.18 (40.33)	−8.41 (0.33)	75.31 (16.19)	66.90 (16.19)	**−46.28 (43.47)**	−50.33 (7.61)	4.06 (44.14)
TBZ	−8.24 (17.74)	−106.82 (11.42)	1.34 (34.69)	−113.72 (38.33)	−8.33 (0.46)	69.91 (18.74)	61.59 (18.74)	**−52.13 (42.68)**	−44.31 (4.02)	−7.82 (42.89)
BZH^+	−251.29 (11.63)	−97.15 (9.62)	5.19 (32.59)	−343.26 (35.94)	−7.87 (0.17)	297.20 (7.78)	271.33 (7.78)	**−71.92 (36.78)**	−50.25 (4.52)	−21.67 (37.07)
$ABZH^+$	−225.18 (16.78)	−129.54 (11.80)	4.81 (35.19)	−349.91 (40.71)	−10.33 (0.25)	267.19 (16.11)	256.86 (16.11)	**−93.05 (39.37)**	−68.62 (4.85)	−24.43 (39.66)
$CBZH^+$	−226.31 (11.97)	−111.38 (10.96)	5.73 (35.19)	−331.96 (38.74)	−8.45 (0.21)	264.22 (7.78)	255.77 (7.78)	**−76.19 (39.50)**	−52.30 (2.01)	−23.89 (39.54)
$FBZH^+$	−223.55 (10.75)	−114.39 (10.21)	5.56 (33.68)	−332.38 (36.82)	−8.66 (0.21)	258.70 (8.12)	250.04 (8.12)	**−82.34 (37.70)**	−50.67 (2.64)	−31.67 (37.78)
$TBZH^+$	−218.87 (11.13)	−115.23 (11.30)	4.77 (35.40)	−329.32 (38.79)	−8.70 (0.38)	255.94 (10.08)	247.23 (10.08)	**−82.09 (40.08)**	−51.17 (2.34)	−30.92 (40.17)

Standard deviations are in parentheses

ΔE_{ELE} and ΔE_{VDW} electrostatic and van der Waals energies as calculated from the MM force field, ΔE_{INT} internal energy arising from bond, angle, and dihedral terms in the MM force field, ΔE_{GAS} total gas phase energy (sum of ΔE_{ELE}, ΔE_{VDW}, and ΔE_{INT}), ΔG_{NP} non-polar contribution to the solvation Gibbs energy, ΔG_{PB} electrostatic contribution to the solvation Gibbs energy, ΔG_{SOLV} sum of non-polar and polar contributions to solvation ($\Delta G_{\mathrm{NP}}+\Delta G_{\mathrm{PB}}$), ΔG estimated binding Gibbs energy calculated as sum of the ΔE_{GAS} and ΔG_{SOLV}, ΔG_{TOT} estimated binding Gibbs energy including the entropic term ($T\Delta S$)

ion–dipole interactions with the host (Fig. 1). Similar observations were found for fluctuations of the van der Waals contribution to the complex stability.

The calculated binding Gibbs energy (ΔG) values, excluding the entropic contribution ($T\Delta S$), were in a good agreement with the experimental ones (see Fig. 2). Including the $T\Delta S$ term disrupted the agreement, presumably due to the inherent inaccuracy of the normal mode analysis. Although the MM-PBSA method employs a continuum solvation model, thereby neglecting the specific solute–solvent interactions important for a proper estimation of the Gibbs energies, the simulation nevertheless correctly predicted the significant increase in binding Gibbs energies of the protonated species and the selectivity of CB toward cationic species.

6 DFT Results

The preferential binding of CB7 with the protonated species results in larger shifts in their pK_a values when compared with their neutral counterparts. In order to predict the binding affinities and the complexation-induced pK_a shifts, we carried out DFT

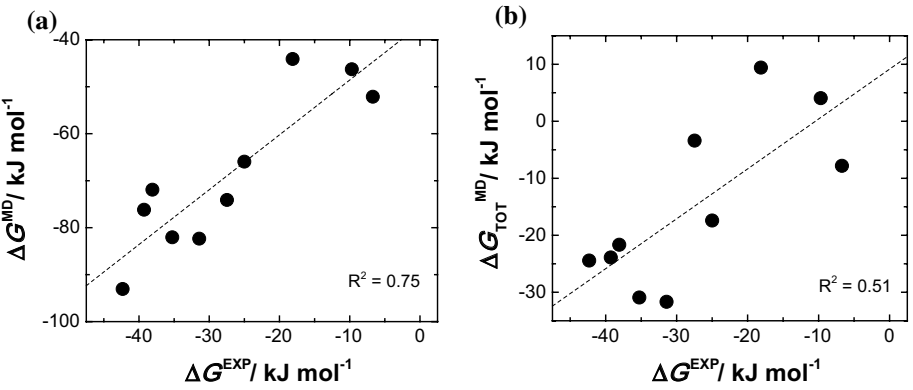

Fig. 2 MD-calculated versus experimental binding energy: **a** ΔG and **b** ΔG_{TOT}

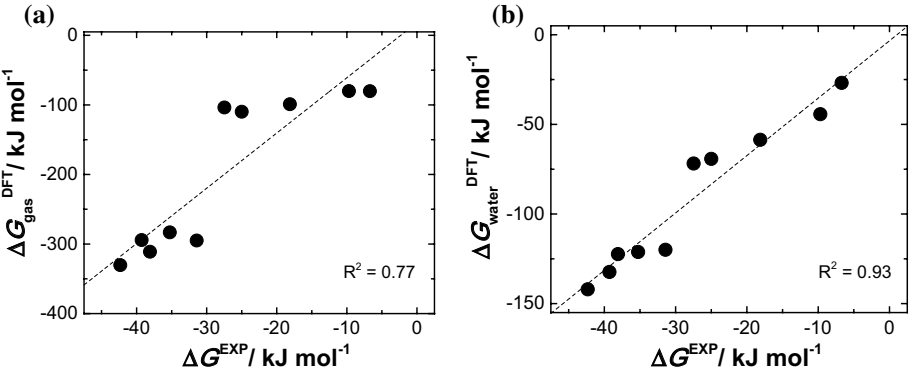

Fig. 3 DFT-calculated versus experimental binding Gibbs energies: **a** in gas-phase and **b** in water

calculations (at the level of wb97xd/6-31G*) in implicit water using the polarizable continuum mode (PCM). The calculated binding Gibbs energies produced better agreement with the experimental trend than MM-PBSA (Fig. 3). Including the effect of solvation had a positive overall impact on the calculated binding trend. The pK_a estimates (Table 3) are in good agreement with the experimental values for the free guests but

Table 3 pK_a values of benzimidazole derivatives in their free pK_a(free) and CB7-complexed pK_a(comp.) states in water, obtained from DFT calculations (PCM)

Guest	Experimental[a]			DFT		
	pK_a(free)	pK_a(comp.)	ΔpK_a	pK_a(free)	pK_a(comp.)	ΔpK_a
ABZ	3.5	6.1	2.6	3.04	15.34	12.3
CBZ	4.5	7.0	2.5	5.95	17.01	11.06
FBZ	4.8	8.6	3.8	6.53	19.78	13.25
TBZ	4.6	8.6	4.0	6.44	22.97	16.53
BZ	5.5	9.0	3.5	5.71	16.88	11.17

[a]Obtained from Reference [18]

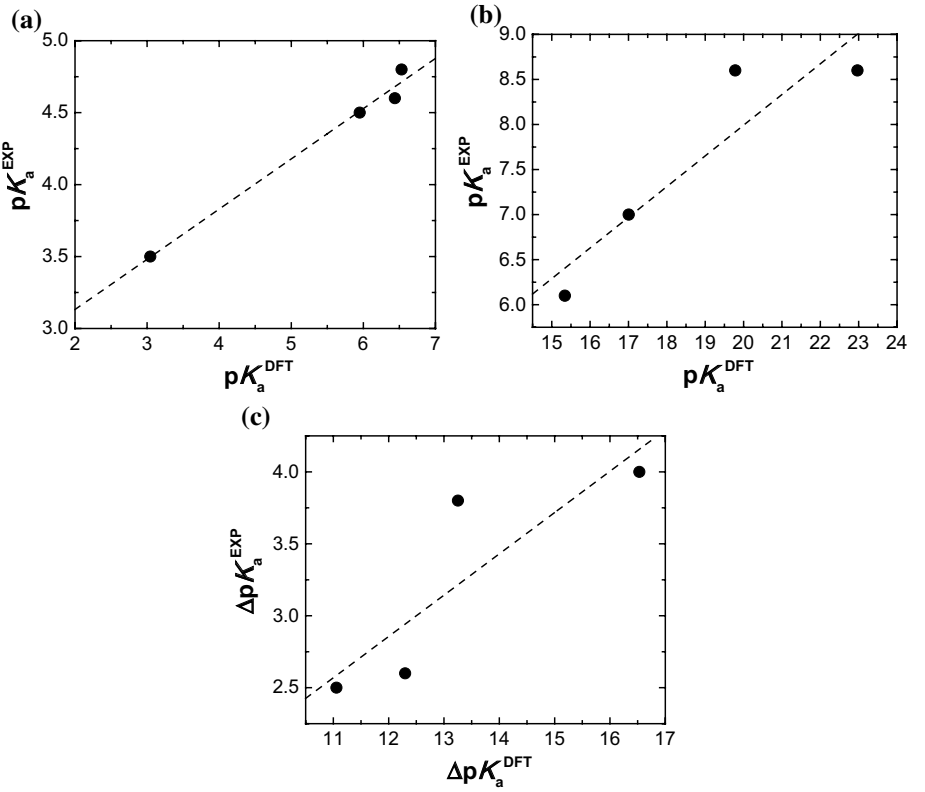

Fig. 4 Experimental versus DFT values for pK_a of the free guests (**a**) and complexed guests (**b**); experimental versus DFT pK_a shifts upon complexation (**c**). Data for BZ are omitted

overestimated them in the case of their complexes. Several factors could contribute to this disagreement: the choice of the basis set, the use of the continuum solvation model, especially for protonated species, which overestimates the binding energies and, as a consequence, exaggerates the pK_a values for complexes, and finally, the use of optimized geometries only and the neglect of the conformational flexibility of the inclusion complexes. However, as Fig. 4 shows, the computed ΔpK_a values (aside from the BZ compound) are in fair agreement with the experimental trend.

7 Conclusion

MD simulations were carried out to study the dynamics and stability of the complexes formed in aqueous solution between CB7 and the protonated and neutral forms of benzimidazole derivatives. The obtained complex geometries formed by CBZ, TBZ, and FBZ exhibit complete encapsulation of the hydrophobic benzene ring within the hydrophobic cavity of CB7, allowing maximum van der Waals interaction. The ABZ complex on the other hand has the hydrophobic propyl-thio moiety included instead. The large binding-induced pK_a shifts reported in the literature are explained by the MM-PBSA results, which demonstrate the preferential binding of CB7 to the protonated guests. DFT results reproduced the experimental trend of the binding strengths and pK_a shifts for the studied molecules but not the absolute values of the pK_a.

References

1. Freeman, W.A., Mock, W.L., Shih, N.Y.: Cucurbituril. J. Am. Chem. Soc. **103**(24), 7367–7368 (1981). https://doi.org/10.1021/ja00414a070
2. Kim, J., Jung, I.-S., Kim, S.-Y., Lee, E., Kang, J.-K., Sakamoto, S., Yamaguchi, K., Kim, K.: New cucurbituril homologues: syntheses, isolation, characterization, and x-ray crystal structures of cucurbit[n]uril (x = 5, 7, and 8). J. Am. Chem. Soc. **122**(3), 540–541 (2000). https://doi.org/10.1021/ja993376p
3. Lee, J.W., Samal, S., Selvapalam, N., Kim, H.-J., Kim, K.: Cucurbituril homologues and derivatives: new opportunities in supramolecular chemistry. Acc. Chem. Res. **36**(8), 621–630 (2003). https://doi.org/10.1021/ar020254k
4. Lagona, J., Mukhopadhyay, P., Chakrabarti, S., Isaacs, L.: The cucurbit[n]uril family. Angew. Chem. Int. Ed. **44**(31), 4844–4870 (2005). https://doi.org/10.1002/anie.200460675
5. Márquez, C., Hudgins, R.R., Nau, W.M.: Mechanism of host–guest complexation by cucurbituril. J. Am. Chem. Soc. **126**(18), 5806–5816 (2004). https://doi.org/10.1021/ja0319846
6. Florea, M., Nau, W.M.: Strong binding of hydrocarbons to cucurbituril probed by fluorescent dye displacement: a supramolecular gas-sensing ensemble. Angew. Chem. Int. Ed. **50**(40), 9338–9342 (2011). https://doi.org/10.1002/anie.201104119
7. Mock, W.L., Shih, N.Y.: Structure and selectivity in host–guest complexes of cucurbituril. J. Org. Chem. **51**(23), 4440–4446 (1986). https://doi.org/10.1021/jo00373a018
8. Assaf, K.I., Nau, W.M.: Cucurbiturils as fluorophilic receptors. Supramol. Chem. **26**, 657–669 (2014). https://doi.org/10.1080/10610278.2014.929130
9. Assaf, K.I., Nau, W.M.: Cucurbiturils: from synthesis to high-affinity binding and catalysis. Chem. Soc. Rev. **44**(2), 394–418 (2015). https://doi.org/10.1039/c4cs00273c
10. Barrow, S.J., Kasera, S., Rowland, M.J., del Barrio, J., Scherman, O.A.: Cucurbituril-based molecular recognition. Chem. Rev. **115**(22), 12320–12406 (2015). https://doi.org/10.1021/acs.chemrev.5b00341
11. Cao, L.P., Sekutor, M., Zavalij, P.Y., Mlinaric-Majerski, K., Glaser, R., Isaacs, L.: Cucurbit[7]uril guest pair with an attomolar dissociation constant. Angew. Chem. Int. Ed. **53**(4), 988–993 (2014). https://doi.org/10.1002/anie.201309635
12. Masson, E., Ling, X.X., Joseph, R., Kyeremeh-Mensah, L., Lu, X.Y.: Cucurbituril chemistry: a tale of supramolecular success. RSC Adv. **2**(4), 1213–1247 (2012). https://doi.org/10.1039/C1ra00768h

13. Ghosh, I., Nau, W.M.: The strategic use of supramolecular p*K*a shifts to enhance the bioavailability of drugs. Adv. Drug Deliv. Rev. **64**(9), 764–783 (2012). https://doi.org/10.1016/j.addr.2012.01.015
14. Danaher, M., De Ruyck, H., Crooks, S.R.H., Dowling, G., O'Keeffe, M.: Review of methodology for the determination of benzimidazole residues in biological matrices. J. Chromatogr. B **845**(1), 1–37 (2007). https://doi.org/10.1016/j.jchromb.2006.07.046
15. Tang, B., Wang, X., Liang, H., Jia, B., Chen, Z.: Study on the supramolecular interaction of thiabendazole and β-cyclodextrin by spectrophotometry and its analytical application. J. Agric. Food Chem. **53**(22), 8452–8459 (2005). https://doi.org/10.1021/jf051683a
16. Melo, M.J., Maçanita, A.L., Melo, E., Wamhoff, H., Pina, F.: Photophysical properties and photodegradation mechanism of 2-(2′-furanyl)-1H-benzimidazole (fuberidazole). J. Photochem. Photobiol. A Chemistry **83**(3), 237–244 (1994). https://doi.org/10.1016/1010-6030(94)03831-7
17. MacGillivray, B.C., Macartney, D.H.: Complexations of the hydrophilic and hydrophobic moieties of benzethonium chloride by cucurbit[7]uril in aqueous solution. Can. J. Chem. **90**(10), 851–857 (2012). https://doi.org/10.1139/v2012-078
18. Koner, A.L., Ghosh, I., Saleh, N.I., Nau, W.M.: Supramolecular encapsulation of benzimidazole-derived drugs by cucurbit[7]uril. Can. J. Chem. **89**(2), 139–147 (2011). https://doi.org/10.1139/V10-079
19. Shaikh, M., Dutta Choudhury, S., Mohanty, J., Bhasikuttan, A.C., Nau, W.M., Pal, H.: Modulation of excited-state proton transfer of 2-(2′-hydroxyphenyl)benzimidazole in a macrocyclic cucurbit[7]uril host cavity: dual emission behavior and p*K*a shift. Chem. Eur. J. **15**(45), 12362–12370 (2009). https://doi.org/10.1002/chem.200900390
20. Saleh, N., Koner, A.L., Nau, W.M.: Activation and stabilization of drugs by supramolecular p*K*(a) shifts: drug-delivery applications tailored for cucurbiturils. Angew. Chem. Int. Ed. **47**(29), 5398–5401 (2008). https://doi.org/10.1002/anie.200801054
21. El-Barghouthi, M.I., Assaf, K.I., Rawashdeh, A.M.M.: Molecular dynamics of methyl viologen–cucurbit[*n*]uril complexes in aqueous solution. J. Chem. Theory Comput. **6**(4), 984–992 (2010). https://doi.org/10.1021/ct900622h
22. Malhis, L.D., Bodoor, K., Assaf, K.I., Al-Sakhen, N.A., El-Barghouthi, M.I.: Molecular dynamics simulation of a cucurbituril based molecular switch triggered by pH changes. Compt. Theor. Chem. **1066**, 104–112 (2015). https://doi.org/10.1016/j.comptc.2015.05.010
23. El-Barghouthi, M.I., Abdel-Halim, H.M., Haj-Ibrahim, F.J., Bodoor, K., Assaf, K.I.: Molecular dynamics of nor-seco-cucurbit[10]uril complexes. J. Incl. Phenom. Macrocycl. Chem. **82**(3), 323–333 (2015). https://doi.org/10.1007/s10847-015-0488-9
24. El-Barghouthi, M.I., Abdel-Halim, H.M., Haj-Ibrahim, F.J., Assaf, K.I.: Molecular dynamics simulation study of the structural features and inclusion capacities of cucurbit[6]uril derivatives in aqueous solutions. Supramol. Chem. **27**(1–2), 80–89 (2015). https://doi.org/10.1080/10610278.2014.910601
25. Chen, S., Han, Z., Zhang, D., Zhan, J.: Theoretical study of the inclusion complexation of TCDD with cucurbit[n]urils. RSC Adv. **4**(94), 52415–52422 (2014). https://doi.org/10.1039/C4RA06011C
26. Gilson, M.K.: Stress analysis at the molecular level: a forced cucurbituril–guest dissociation pathway. J. Chem. Theory Comput. **6**(3), 637–646 (2010). https://doi.org/10.1021/ct900668k
27. Fileti, E., Colherinhas, G., Malaspina, T.: Predicting the properties of a new class of host–guest complexes: C60 fullerene and CB[9] cucurbituril. Phys. Chem. Chem. Phys. **16**(41), 22823–22829 (2014). https://doi.org/10.1039/C4CP03299C
28. Fenley, A.T., Henriksen, N.M., Muddana, H.S., Gilson, M.K.: Bridging calorimetry and simulation through precise calculations of cucurbituril–guest binding enthalpies. J. Chem. Theory Comput. **10**(9), 4069–4078 (2014). https://doi.org/10.1021/ct5004109
29. Venkataramanan, N.S., Ambigapathy, S.: Encapsulation of sulfur, oxygen, and nitrogen mustards by cucurbiturils: a DFT study. J. Incl. Phenom. Macrocycl. Chem. **83**(3–4), 387–400 (2015). https://doi.org/10.1007/s10847-015-0575-y
30. Kim, M.O., Blachly, P.G., Kaus, J.W., McCammon, J.A.: Protocols utilizing constant pH molecular dynamics to compute pH-dependent binding free energies. J. Phys. Chem. B **119**(3), 861–872 (2015). https://doi.org/10.1021/jp505777n
31. Fatiha, M., Faiza, B., Ichraf, K., Leila, N., Eddine, K.D.: TD-DFT calculations of visible spectra and structural studies of carbendazim inclusion complex with cucurbit[7]uril. J. Taiwan Inst. Chem. Eng. **50**(Supplement C), 37–42 (2015). https://doi.org/10.1016/j.jtice.2014.12.007
32. Shewale, M.N., Lande, D.N., Gejji, S.P.: Encapsulation of benzimidazole derivatives within cucurbit[7]uril: Density functional investigations. J. Mol. Liq. **216**(Supplement C), 309–317 (2016). https://doi.org/10.1016/j.molliq.2015.12.076
33. Case, D.A., Darden, T.A., Cheatham III, T.E., Simmerling, C.L., Wang, J., Duke, R.E., Luo, R., Walker, R.C., Zhang, W., Merz, K.M., Roberts, B., Wang, B., Hayik, S., Roitberg, A., Seabra, G.,

Kolossváry, I., Wong, K.F., Paesani, F., Vanicek, J., Liu, J., Wu, X., Brozell, S.R., Steinbrecher, T., Gohlke, H., Cai, Q., Ye, X., Wang, J., Hsieh, M.-J., Cui, G., Roe, D.R., Mathews, D.H., Seetin, M.G., Sagui, C., Babin, V., Luchko, T., Gusarov, S., Kovalenko, A., Kollman, P.A.: AMBER 11. University of California, San Francisco (2010)

34. Wang, J., Wolf, R.M., Caldwell, J.W., Kollman, P.A., Case, D.A.: Development and testing of a general amber force field. J. Comput. Chem. **25**(9), 1157–1174 (2004). https://doi.org/10.1002/jcc.20035
35. Bayly, C.I., Cieplak, P., Cornell, W., Kollman, P.A.: A well-behaved electrostatic potential based method using charge restraints for deriving atomic charges: the RESP model. J. Phys. Chem. **97**(40), 10269–10280 (1993). https://doi.org/10.1021/j100142a004
36. Jorgensen, W.L., Chandrasekhar, J., Madura, J.D., Impey, R.W., Klein, M.L.: Comparison of simple potential functions for simulating liquid water. J. Chem. Phys. **79**(2), 926–935 (1983). https://doi.org/10.1063/1.445869
37. York, D.M., Darden, T.A., Pedersen, L.G.: The effect of long-range electrostatic interactions in simulations of macromolecular crystals: a comparison of the Ewald and truncated list methods. J. Chem. Phys. **99**(10), 8345–8348 (1993). https://doi.org/10.1063/1.465608
38. Ryckaert, J.-P., Ciccotti, G., Berendsen, H.J.C.: Numerical integration of the Cartesian equations of motion of a system with constraints: molecular dynamics of *n*-alkanes. J. Comput. Phys. **23**(3), 327–341 (1977). https://doi.org/10.1016/0021-9991(77)90098-5
39. Humphrey, W., Dalke, A., Schulten, K.: VMD: visual molecular dynamics. J. Mol. Graphics **14**(1), 33–38 (1996). https://doi.org/10.1016/0263-7855(96)00018-5
40. Rawashdeh, A.M.M., El-Barghouthi, M.I., Assaf, K.I., Al-Gharabli, S.I.: Complexation of *N*-methyl-4-(*p*-methyl benzoyl)-pyridinium methyl cation and its neutral analogue by cucurbit[7]uril and beta-cyclodextrin: a computational study. J. Incl. Phenom. Macrocycl. Chem. **64**(3–4), 357–365 (2009). https://doi.org/10.1007/s10847-009-9574-1
41. Frisch, M.J., Trucks, G.W., Schlegel, H.B., Scuseria, G.E., Robb, M.A., Cheeseman, J.R., Scalmani, G., Barone, V., Mennucci, B., Petersson, G.A., Nakatsuji, H., Caricato, M., Li, X., Hratchian, H.P., Izmaylov, A.F., Bloino, J., Zheng, G., Sonnenberg, J.L., Hada, M., Ehara, M., Toyota, K., Fukuda, R., Hasegawa, J., Ishida, M., Nakajima, T., Honda, Y., Kitao, O., Nakai, H., Vreven, T., Montgomery, J.A., Peralta, J.E., Ogliaro, F., Bearpark, M., Heyd, J.J., Brothers, E., Kudin, K.N., Staroverov, V.N., Kobayashi, R., Normand, J., Raghavachari, K., Rendell, A., Burant, J.C., Iyengar, S.S., Tomasi, J., Cossi, M., Rega, N., Millam, J.M., Klene, M., Knox, J.E., Cross, J.B., Bakken, V., Adamo, C., Jaramillo, J., Gomperts, R., Stratmann, R.E., Yazyev, O., Austin, A.J., Cammi, R., Pomelli, C., Ochterski, J.W., Martin, R.L., Morokuma, K., Zakrzewski, V.G., Voth, G.A., Salvador, P., Dannenberg, J.J., Dapprich, S., Daniels, A.D., Farkas, Foresman, J.B., Ortiz, J.V., Cioslowski, J., Fox, D.J.: Gaussian 09, Revision B.01. Gaussian, Inc., Wallingford (2009)
42. Muckerman, J.T., Skone, J.H., Ning, M., Wasada-Tsutsui, Y.: Toward the accurate calculation of p*K*a values in water and acetonitrile. Biochim. Biophys. Acta **1827**(8), 882–891 (2013). https://doi.org/10.1016/j.bbabio.2013.03.011
43. Assaf, K.I., Qaroush, A.K., Eftaiha, E.A.F.: New insights into the chemistry of ionic alkylorganic carbonates: a computational study. Phys. Chem. Chem. Phys. **19**(23), 15403–15411 (2017). https://doi.org/10.1039/C7CP02087B